Supersymmetric Dark Matter Candidates

The lightest neutralino, the gravitino, and the axino

Frank Daniel Steffen[1] [a]

Max-Planck-Institut für Physik, Föhringer Ring 6, D-80805 Munich, Germany

Abstract. In supersymmetric extensions of the Standard Model, the lightest neutralino, the gravitino, and the axino can appear as the lightest supersymmetric particle and as such provide a compelling explanation of the non-baryonic dark matter in our Universe. For each of these dark matter candidates, I review the present status of primordial production mechanisms, cosmological constraints, and prospects of experimental identification.

PACS. 95.35.+d Dark matter – 12.60.Jv Supersymmetric models – 04.65.+e Supergravity

1 Introduction

Numerous astrophysical and cosmological considerations point to the existence of non-baryonic dark matter in our Universe [1,2]. In fact, based on observations of supernovae, galaxy clusters, and the cosmic microwave background (CMB), we believe today that our Universe is flat with about 76%, 20%, and 4% of the critical energy density ρ_c provided in the form of dark energy, non-baryonic dark matter, and baryons, respectively [3,4]. A nominal "3σ" range[1] of the dark matter density $\Omega_{\rm dm} = \rho_{\rm dm}/\rho_c$ can be inferred from measurements of the CMB anisotropies by the Wilkinson Microwave Anisotropy Probe (WMAP) satellite [3]

$$\Omega_{\rm dm}^{3\sigma} h^2 = 0.105^{+0.021}_{-0.030} \tag{1}$$

with $h = 0.73^{+0.04}_{-0.03}$ denoting the Hubble constant in units of $100\,{\rm km\,Mpc^{-1}s^{-1}}$.

Relying on the pieces of evidence, we think that a particle physics candidate for dark matter has to be electrically neutral, color neutral,[2] and stable or have a lifetime $\tau_{\rm dm}$ that is not much smaller than the age of the Universe today $t_0 \simeq 14$ Gyr. Moreover, the species providing the dominant contribution to $\Omega_{\rm dm}$ have to be sufficiently slow to allow for structure formation. For example, since the neutrinos of the Standard Model are too light, $\sum_i m_{\nu_i} \lesssim \mathcal{O}(1\text{ eV})$ [6], they were too fast at early times. Accordingly, they are classified as hot dark matter which can constitute only a minor fraction of $\Omega_{\rm dm}$ since otherwise structure formation cannot be understood [7]. Thus, the observationally inferred dark matter density can be considered as evidence for physics beyond the Standard Model.

Supersymmetric (SUSY) extensions of the Standard Model are an appealing concept because of their remarkable properties, for example, with respect to gauge coupling unification, the hierarchy problem, and the embedding of gravity [8,9,10,11,12,13]. As superpartners of the Standard Model particles, new particles appear including fields that are electrically neutral and color neutral. Since they have not been detected at particle accelerators, these sparticles must be heavy or extremely weakly interacting.

Because of the non-observation of reactions that violate lepton number L or baryon number B, it is often assumed—as also in this review—that SUSY theories respect the multiplicative quantum number

$$\mathrm{R} = (-1)^{3B+L+2S}\,, \tag{2}$$

known as R-parity, with S denoting the spin. Since Standard Model particles and superpartners carry respectively even (+1) and odd (-1) R-parity, its conservation implies that superpartners can only be produced or annihilated in pairs and that the lightest supersymmetric particle (LSP) cannot decay even if it is heavier than most (or all) of the Standard Model particles.[3] An electrically neutral and color neutral LSP can thus be a compelling dark matter candidate. For the lightest neutralino, the gravitino, and the axino, which are well-motivated LSP candidates, this is shown below. For each scenario, I will address implications for cosmology and experimental prospects. Note that the

[a] *Email:* steffen@mppmu.mpg.de

[1] Note that the nominal "3σ" range is derived assuming a restrictive six-parameter "vanilla" model. A larger range is possible—even with additional data from other cosmological probes—if the fit is performed in the context of a more general model that includes other physically motivated parameters such as a nonzero neutrino mass [5]. Thereby, the range $0.094 < \Omega_{\rm dm}h^2 < 0.136$ has been obtained in Ref. [5].

[2] A colored dark matter candidate is disfavored by severe limits from searches for anomalous heavy nuclei [4].

[3] While R-parity conservation is assumed in this review, its violation is a realistic option; see, e.g., [14,15,16,17,18].

discussion of gravitino/axino dark matter in Sects. 3 and 4 will be more extensive than the one of neutralino dark matter in Sect. 2, for which numerous excellent reviews exist such as [19,12,20,21].

2 Neutralino Dark Matter

The lightest neutralino $\widetilde{\chi}_1^0$ appears already in the minimal supersymmetric Standard Model (MSSM) as the lightest mass eigenstate among the four neutralinos being mixtures of the bino $\widetilde{B}$, the wino $\widetilde{W}$, and the neutral higgsinos $\widetilde{H}_u^0$ and $\widetilde{H}_d^0$. Accordingly, $\widetilde{\chi}_1^0$ is a spin 1/2 fermion with weak interactions only. Its mass $m_{\widetilde{\chi}_1^0}$ depends on the gaugino mass parameters M_1 and M_2, on the ratio of the two MSSM Higgs doublet vacuum expectation values $\tan\beta$, and the higgsino mass parameter μ. Expecting $m_{\widetilde{\chi}_1^0} = \mathcal{O}(100\text{ GeV})$, $\widetilde{\chi}_1^0$ is classified as a weakly interacting massive particle (WIMP).

Motivated by theories of grand unification and supergravity [22] and by experimental constraints on flavor mixing and CP violation [4], one often assumes universal soft SUSY breaking parameters at the scale of grand unification M_{GUT}; cf. [11,12,13,20] and references therein. For example, in the framework of the constrained MSSM (CMSSM), the gaugino masses, the scalar masses, and the trilinear scalar interactions are assumed to take on the respective universal values $m_{1/2}$, m_0, and A_0 at M_{GUT}. Specifying $m_{1/2}$, m_0, A_0, $\tan\beta$, and the sign of μ, the low-energy mass spectrum is given by the renormalization group running from M_{GUT} downwards.

Assuming $A_0 = 0$ for simplicity, the lightest Standard Model superpartner—or lightest ordinary superpartner (LOSP)—is either the lightest neutralino $\widetilde{\chi}_1^0$ or the lighter stau $\widetilde{\tau}_1$, whose mass is denoted by $m_{\widetilde{\tau}_1}$. If the LSP is assumed to be the LOSP, the parameter region in which $m_{\widetilde{\tau}_1} < m_{\widetilde{\chi}_1^0}$ is usually not considered because of severe upper limits on the abundance of stable charged particles [4]. However, in gravitino/axino LSP scenarios, in which the LOSP is the next-to-lightest supersymmetric particle (NLSP), the $\widetilde{\tau}_1$ LOSP case is viable and particularly promising for collider phenomenology as will be discussed in Sects. 3 and 4.

In Fig. 1 (from [23]) the dotted (blue in the web version) lines show contours of m_{LOSP} in the $(m_{1/2}, m_0)$ plane for $A_0 = 0$, $\mu > 0$, $\tan\beta = 10$. Above (below) the dashed line, $m_{\widetilde{\chi}_1^0} < m_{\widetilde{\tau}_1}$ ($m_{\widetilde{\tau}_1} < m_{\widetilde{\chi}_1^0}$). The medium gray and the light gray regions at small $m_{1/2}$ are excluded respectively by the mass bounds $m_{\widetilde{\chi}_1^\pm} > 94$ GeV and $m_{\text{H}} > 114.4$ GeV from chargino and Higgs searches at LEP [4]. It can be seen that $m_{\widetilde{\chi}_1^0} = \mathcal{O}(100\text{ GeV})$ appears naturally within the CMSSM.

2.1 Primordial Origin

The $\widetilde{\chi}_1^0$'s were in thermal equilibrium for primordial temperatures of $T > T_{\text{f}} \simeq m_{\widetilde{\chi}_1^0}/20$. At T_{f}, the annihilation rate of the (by then) non-relativistic $\widetilde{\chi}_1^0$'s

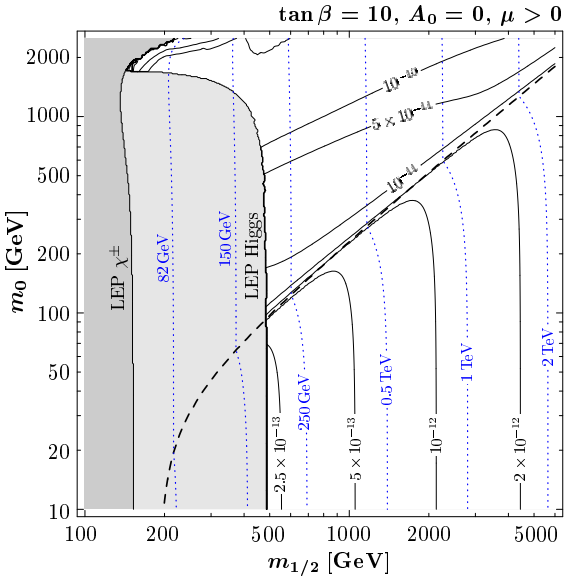

Fig. 1. Contours of m_{LOSP} (dotted blue lines) and $Y_{\text{LOSP}}^{\text{dec}}$ (solid black lines) in the $(m_{1/2}, m_0)$ plane for $A_0 = 0$, $\mu > 0$, $\tan\beta = 10$. Above (below) the dashed line, $m_{\widetilde{\chi}_1^0} < m_{\widetilde{\tau}_1}$ ($m_{\widetilde{\tau}_1} < m_{\widetilde{\chi}_1^0}$). The medium gray and the light gray regions show the LEP bounds $m_{\widetilde{\chi}_1^\pm} > 94$ GeV and $m_{\text{H}} > 114.4$ GeV, respectively [4]. The contours are obtained with the spectrum generator `SuSpect 2.34` [24] using $m_t = 172.5$ GeV and $m_{\text{b}}(m_{\text{b}})^{\overline{\text{MS}}} = 4.23$ GeV, and with `micrOMEGAs 1.37` [25,26]. From [23].

becomes smaller than the Hubble rate so that they decouple from the thermal plasma. Thus, for $T \lesssim T_{\text{f}}$, their yield $Y_{\widetilde{\chi}_1^0} \equiv n_{\widetilde{\chi}_1^0}/s$ is given by $Y_{\widetilde{\chi}_1^0}^{\text{dec}} \approx Y_{\widetilde{\chi}_1^0}^{\text{eq}}(T_{\text{f}})$, where $n_{\widetilde{\chi}_1^0}^{(\text{eq})}$ is the (equilibrium) number density of $\widetilde{\chi}_1^0$'s and $s = 2\pi^2\, g_{*S}\, T^3/45$ the entropy density. Depending on details of the $\widetilde{\chi}_1^0$ decoupling, $Y_{\widetilde{\chi}_1^0}^{\text{dec}}$ is very sensitive to the mass spectrum and the couplings of the superparticles. Indeed, convenient computer programs such as `DarkSUSY` [27] or `micrOMEGAs 1.37` [25,26] are available which allow for a numerical calculation of the LOSP decoupling and the resulting thermal relic abundance in a given SUSY model.

The $Y_{\text{LOSP}}^{\text{dec}}$ contours shown by the solid black lines in Fig. 1 illustrate that the $\widetilde{\chi}_1^0$ LSP yield can easily vary by more than an order of magnitude. Because of this sensitivity, the associated thermal relic density

$$\Omega_{\widetilde{\chi}_1^0} h^2 = m_{\widetilde{\chi}_1^0}\, Y_{\widetilde{\chi}_1^0}^{\text{dec}}\, s(T_0)\, h^2/\rho_c \qquad (3)$$

agrees with $\Omega_{\text{dm}}^{3\sigma} h^2$ only in narrow regions in the parameter space; $\rho_c/[s(T_0)h^2] = 3.6\times10^{-9}\,\text{GeV}$ [4]. This can be seen in Fig. 2 (from [28]) where the black strips indicate the region with $0.087 \le \Omega_{\widetilde{\chi}_1^0} h^2 \le 0.138$.

Remarkably, it is exactly the small width of the $\Omega_{\widetilde{\chi}_1^0} = \Omega_{\text{dm}}$ regions which could help us to identify $\widetilde{\chi}_1^0$ dark matter. Once sparticles are produced at colliders, the data analysis will aim at determinig the SUSY model realized in nature [29,30]. For the reconstructed model, a precise calculation of $\Omega_{\widetilde{\chi}_1^0}$ is possible assuming a standard thermal history of the Universe.

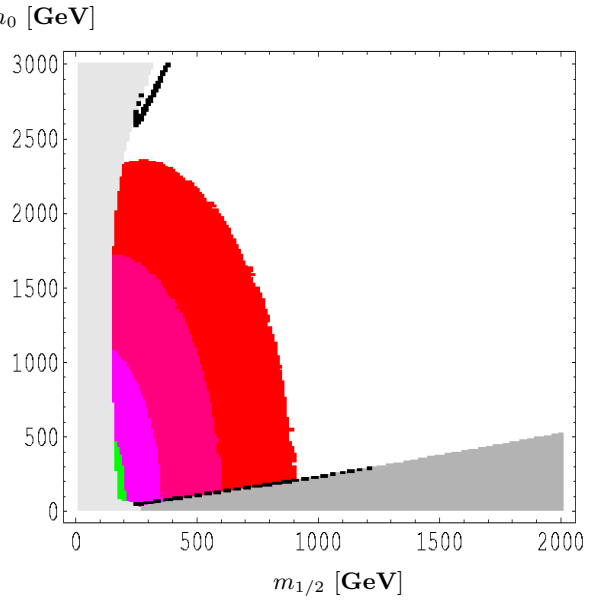

Fig. 2. Regions (black) with $0.087 \leq \Omega_{\widetilde{\chi}^0_1} h^2 \leq 0.138$ in the $(m_{1/2}, m_0)$ plane for $A_0 = 0, \mu > 0$, $\tan\beta = 10$, and $m_t = 172.7$ GeV. In the dark gray triangular region, $m_{\widetilde{\chi}^0_1} > m_{\widetilde{\tau}_1}$. The light gray region at small $m_{1/2}$ is excluded by the requirement of correct electroweak symmetry breaking or by sparticle search limits [28], the two medium shaded (light pink in the web version) bands by the LEP bound $m_{\rm H} > 114$ GeV, and the small light shaded (green in the web version) spot by the $b \to s\gamma$ constraint: $2.65 \leq {\rm BR}(b \to s\gamma)/10^{-4} \leq 4.45$. The dark shaded (red in the web version) band is compatible with having a Standard Model like Higgs boson near 115 GeV. From [28].

Because of the sensitivity of $\Omega_{\widetilde{\chi}^0_1}$ with respect to the SUSY model, an agreement of the obtained $\Omega_{\widetilde{\chi}^0_1}$ with $\Omega_{\rm dm}$ will then be strong evidence for the $\widetilde{\chi}^0_1$ LSP providing $\Omega_{\rm dm}$ and for a standard thermal history up to the $\widetilde{\chi}^0_1$-decoupling temperature $T_{\rm f}$. Since $\widetilde{\chi}^0_1$'s decouple already as a non-relativistic species, it is also guaranteed that they are sufficiently cold to allow for cosmic structure formation.

2.2 Experimental Prospects

For experimental tests of the $\widetilde{\chi}^0_1$ dark matter hypothesis, three complementary techniques exist: indirect, direct, and collider searches. While there is an enormous activity in each of those fields, I will summarize only the main ideas. For more detailed discussions, see [31, 21, 32] and references therein.

Let us first turn to indirect searches. Since dark matter clumps, one expects regions with an increased $\widetilde{\chi}^0_1$ density such as galaxy halos, the center of galaxies, and the center of stars. While $\widetilde{\chi}^0_1$ pair annihilation after $\widetilde{\chi}^0_1$ decoupling is basically negligible for calculations of $\Omega_{\widetilde{\chi}^0_1}$, it should occur at a significant rate in these regions. The resulting Standard Model particles should then lead to energetic cosmic rays and thereby to an excess of photons, neutrinos, positrons, and antiprotons over backgrounds expected from standard cosmic ray models without dark matter annihilation. In fact, data from the Energetic Gamma Ray Experiment Telescope (EGRET) has already been interpreted as evidence for $\widetilde{\chi}^0_1$ annihilation [33, 34] within SUSY models that will be testable in direct and collider searches. For a discussion of these and other potential hints, see [35, 21] and references therein.

In direct searches, one looks for signals of $\widetilde{\chi}^0_1$'s—or more generally WIMPs—passing through earth that scatter elastically off nuclei. Being located in environments deep underground that are well shielded against unwanted background, an enormous sensitivity has already been reached [36, 37, 38, 39]. Since no unambiguous signal of a $\widetilde{\chi}^0_1$–nucleus scattering event has been observed so far, $m_{\widetilde{\chi}^0_1}$-dependent upper limits on the respective $\widetilde{\chi}^0_1$ cross section are obtained. Indeed, the current best limits given by the CDMS II [38] and the Xenon 10 [39] experiments exclude already a part of the SUSY parameter space; see, for example, [20, 21, 32] and references therein. These limits, however, depend on the assumed $\widetilde{\chi}^0_1$ flux at the detector location, which is subject to significant uncertainties due to possible inhomogeneities in the dark matter distribution in galaxies. Such inhomogeneities should manifest themselves also in indirect searches which can help to reduce those uncertainties. Once $\widetilde{\chi}^0_1$ events are observed in direct searches, one can succeed in reconstructing the $\widetilde{\chi}^0_1$ velocity distribution [40]. By analyzing the recoil spectra, $m_{\widetilde{\chi}^0_1}$ can even be estimated in a way that is independent of the dark matter density on earth [41].

In most searches for SUSY at colliders, it is assumed that R-parity is conserved. Accordingly, one expects that superpartners are produced in pairs before decaying via cascades into the LSP and energetic fermions. As a weakly-interacting particle, every $\widetilde{\chi}^0_1$ LSP produced will escape the detector without leaving a track. Thus, the existence of SUSY and the $\widetilde{\chi}^0_1$ LSP has to be inferred from studies of missing transverse energy $E_T^{\rm miss}$ and energetic jets and leptons emitted along the cascades. Along these lines, ongoing investigations are pursued based on data from $p\bar{p}$ collisions with a center-of-mass energy of $\sqrt{s} = 2$ TeV at the Fermilab Tevatron Collider. While lower limits on the masses of squarks and gluinos have been extracted, no evidence for SUSY or the $\widetilde{\chi}^0_1$ LSP has been reported so far [42, 43]. With the first pp collisions with $\sqrt{s} = 14$ TeV at the CERN Large Hadron Collider (LHC) expected in the year 2008, there are high hopes that the new energy range will allow for a copious production of superpartners. Here large $E_T^{\rm miss}$ will be the key quantity for early SUSY searches [44, 45]. Despite an enormous potential for mass and spin measurements of SUSY particles at the LHC [46], additional precision studies at the planned International Linear Collider (ILC) [47, 48] appear to be crucial for the identification of the $\widetilde{\chi}^0_1$ LSP [31, 49].

3 Gravitino Dark Matter

The gravitino $\widetilde{G}$ appears (as the spin-3/2 superpartner of the graviton) once SUSY is promoted from a global to a local symmetry leading to supergravity [8]. The gravitino mass $m_{\widetilde{G}}$ depends strongly on the SUSY-breaking scheme and can range from the eV scale to scales beyond the TeV region [9,11,50,51,52,53,54,55]. For example, in gauge-mediated SUSY breaking schemes [50,51,52], the mass of the gravitino is typically less than 1 GeV, while in gravity-mediated schemes [9,11] it is expected to be in the GeV to TeV range. The gravitino is a singlet with respect to the gauge groups of the Standard Model. Its interactions—given by the supergravity Lagrangian [56,8]—are suppressed by the (reduced) Planck scale [4]

$$\mathrm{M_P} = 2.4 \times 10^{18}\,\mathrm{GeV}\,. \tag{4}$$

Once SUSY is broken, the extremely weak gravitino interactions are enhanced through the super-Higgs mechanism, in particular, at energy/mass scales that are large with respect to $m_{\widetilde{G}}$. Nevertheless, the gravitino can be classified as an extremely weakly interacting particle (EWIP). It must not be massive since even a light gravitino can evade its production at colliders because of its tiny interaction strength. Considering the case of the $\widetilde{G}$ LSP, in which the LOSP is the unstable NLSP that decays eventually into the $\widetilde{G}$ LSP, $m_{\tilde{\tau}_1} < m_{\widetilde{\chi}^0_1}$ (cf. Fig. 1) is viable as already mentioned.[4]

3.1 Primordial Origin

Assuming that inflation governed the earliest moments of the Universe, any initial population of gravitinos must be diluted away by the exponential expansion during the slow-roll phase. Indeed, gravitinos are typically not in thermal equilibrium with the primordial plasma after inflation because of their extremely weak interactions.[5] At high temperatures, however, they can be produced efficiently in thermal scattering of particles in the primordial plasma. Derived in a consistent gauge-invariant treatment, the resulting thermally produced (TP) gravitino density reads [64,65]

$$\Omega^{\mathrm{TP}}_{\widetilde{G}} h^2 = \sum_{i=1}^{3} \omega_i\, g_i^2 \left(1 + \frac{M_i^2}{3m^2_{\widetilde{G}}}\right) \ln\left(\frac{k_i}{g_i}\right) \times \left(\frac{m_{\widetilde{G}}}{100\ \mathrm{GeV}}\right)\left(\frac{T_\mathrm{R}}{10^{10}\,\mathrm{GeV}}\right)\,, \tag{5}$$

with ω_i, the gauge couplings g_i, the gaugino mass parameters M_i, and k_i as given in Table 1. Here M_i and g_i are understood to be evaluated at the reheating temperature[6] after inflation T_R [65].[7] For the case of universal $M_{1,2,3} = m_{1/2}$ at M_GUT and $m_{\widetilde{G}} \ll M_i$, i.e., $(1 + M_i^2/3m^2_{\widetilde{G}}) \simeq M_i^2/3m^2_{\widetilde{G}}$, $\Omega^{\mathrm{TP}}_{\widetilde{G}} h^2$ can be approximated by the convenient expression [67]

$$\Omega^{\mathrm{TP}}_{\widetilde{G}} h^2 \simeq 0.32\Big(\frac{10\ \mathrm{GeV}}{m_{\widetilde{G}}}\Big)\Big(\frac{m_{1/2}}{1\ \mathrm{TeV}}\Big)^2\Big(\frac{T_\mathrm{R}}{10^8\ \mathrm{GeV}}\Big). \tag{6}$$

The thermally produced gravitinos do not affect the thermal evolution of the LOSP (or NLSP) prior to its decay which occurs typically after decoupling from the thermal plasma. Moreover, since each NLSP decays into one $\widetilde{G}$ LSP, the NLSP decay leads to a non-thermally produced (NTP) gravitino density [68,69,70,71]

$$\Omega^{\mathrm{NTP}}_{\widetilde{G}} h^2 = m_{\widetilde{G}}\, Y^{\mathrm{dec}}_{\mathrm{NLSP}}\, s(T_0) h^2/\rho_\mathrm{c} \tag{7}$$

so that the guaranteed density is given by[8]

$$\Omega_{\widetilde{G}} h^2 = \Omega^{\mathrm{TP}}_{\widetilde{G}} h^2 + \Omega^{\mathrm{NTP}}_{\widetilde{G}} h^2\,. \tag{8}$$

While $\Omega^{\mathrm{TP}}_{\widetilde{G}}$ is sensitive to M_i and T_R for a given $m_{\widetilde{G}}$, $\Omega^{\mathrm{NTP}}_{\widetilde{G}}$ depends on $Y^{\mathrm{dec}}_{\mathrm{NLSP}} = Y^{\mathrm{dec}}_{\mathrm{LOSP}}$ and thereby on details of the SUSY model realized in nature; cf. Sect. 2.1. For the case of the $\widetilde{\tau}_1$ NLSP, simple approximations can be used such as [69,74,75]

$$Y^{\mathrm{dec}}_{\widetilde{\tau}_1} \simeq 0.7 \times 10^{-12}\left(\frac{m_{\widetilde{\tau}_1}}{1\ \mathrm{TeV}}\right) \tag{9}$$

which is valid outside of the $\widetilde{\tau}_1$–$\widetilde{\chi}^0_1$ coannihilation region for a spectrum in which $m_{\widetilde{\tau}_1}$ is significantly below the masses of the lighter selectron and the lighter smuon, $m_{\widetilde{\tau}_1} \ll m_{\widetilde{e}_1,\widetilde{\mu}_1}$, and in which $\widetilde{\chi}^0_1 \simeq \widetilde{B}$ with a mass of $m_{\widetilde{B}} = 1.1\, m_{\widetilde{\tau}_1}$.[9] Scenarios with $\Omega_{\widetilde{G}} = \Omega_\mathrm{dm}$ are

[4] A stop $\widetilde{t}_1$ NLSP is not feasible in the CMSSM [57].

[5] In gauge-mediated SUSY breaking scenarios, light gravitinos can be viable thermal relics if their abundance is diluted by entropy production, which can result, for example, from decays of messenger fields [58,59,60,61,62,63].

[6] For a discussion on the T_R definition, see Sec. 2 in [23].

[7] Note that the field-theoretical methods applied in the derivation of (5) [64,65] require weak couplings $g_i \ll 1$ and thus $T \gg 10^6$ GeV. For an alternative approach, see [66].

[8] In this review I do not discuss gravitino production from inflaton decays which can be substantial depending on the inflation model; see, e.g., [72,73].

[9] The $Y^{\mathrm{dec}}_{\mathrm{LOSP}}$ contours in the $\widetilde{\tau}_1$ LOSP region in Fig. 1, in which $m_{\widetilde{\tau}_1} \lesssim m_{\widetilde{e}_1,\widetilde{\mu}_1} \lesssim 1.1\, m_{\widetilde{\tau}_1}$, illustrate that the $\widetilde{\tau}_1$ LSP yield can be about twice as large for a given $m_{\widetilde{\tau}_1}$ due to slepton coannihilation. Approaching the $\widetilde{\chi}^0_1$–$\widetilde{\tau}_1$ coannihilation region, $m_{\widetilde{\chi}^0_1} \approx m_{\widetilde{\tau}_1}$, even larger factors occur.

Table 1. Assignments of the index i, the gauge coupling g_i, and the gaugino mass parameter M_i to the gauge groups $\mathrm{U(1)_Y}$, $\mathrm{SU(2)_L}$, and $\mathrm{SU(3)_c}$, and the constants ω_i and k_i.

gauge group	i	g_i	M_i	ω_i	k_i
$\mathrm{U(1)_Y}$	1	g'	M_1	0.018	1.266
$\mathrm{SU(2)_L}$	2	g	M_2	0.044	1.312
$\mathrm{SU(3)_c}$	3	g_s	M_3	0.117	1.271

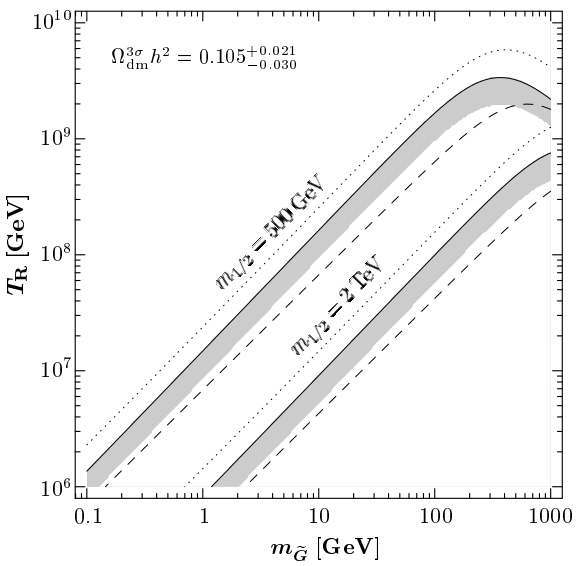

Fig. 3. Upper limits on the reheating temperature $T_{\rm R}$ in the $\widetilde{G}$ LSP case. On the upper (lower) gray band, $\Omega^{\rm TP}_{\widetilde{G}} \in \Omega^{3\sigma}_{\rm dm}$ for $M_{1,2,3} = m_{1/2} = 500$ GeV (2 TeV) at $M_{\rm GUT}$. The corresponding limits from $\Omega^{\rm TP}_{\widetilde{G}}h^2 \leq 0.126$ shown by the dashed and dotted lines are obtained respectively with (5) for $M_1/10 = M_2/2 = M_3 = m_{1/2}$ at $M_{\rm GUT}$ and with the result of Ref. [64] for $M_3 = m_{1/2}$ at $M_{\rm GUT}$. From [23].

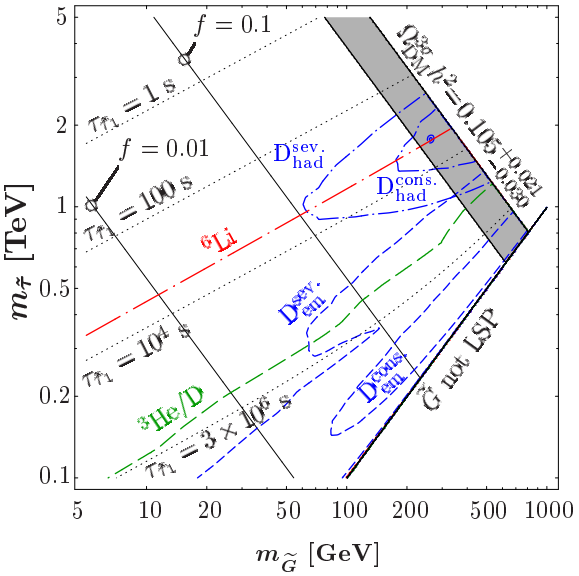

Fig. 4. Cosmological constraints on the masses of the gravitino LSP and a purely 'right-handed' $\widetilde{\tau}_1$ NLSP. The gray band indicates $\Omega^{\rm NTP}_{\widetilde{G}} \in \Omega^{3\sigma}_{\rm dm}$. Above this band, $\Omega_{\widetilde{G}} > 0.126$. Only 10% (1%) of $\Omega_{\rm dm}$ is provided by $\Omega^{\rm NTP}_{\widetilde{G}}$ for scenarios that fall onto the thin solid line labeled by $f = 0.1$ (0.01). The dotted lines show contours of $\tau_{\widetilde{\tau}_1}$. The region below the long-dash-dotted (red in the web version) line and below the long-dashed (green in the web version) line is disfavored by the observationally inferred abundances of primordial ^{6}Li [67] and ^{3}He/D [81]. The effect of electromagnetic and hadronic energy injection on primordial D disfavors the regions inside the short-dash-dotted (blue in the web version) curves and to the right or inside of the short-dashed (blue in the web version) curves, respectively. With (9) and $\epsilon_{\rm em} = 0.3E_\tau$, the curves are obtained from the severe and conservative upper limits defined in Sec. 4.1 of [74] based on results from [82,81].

found for natural mass spectra and for a wide range of $m_{\widetilde{G}}$–$T_{\rm R}$ combinations. This is illustrated in Figs. 3, 4, and 5.

In $\widetilde{G}$ LSP scenarios, upper limits on $T_{\rm R}$ can be derived since $\Omega^{\rm TP}_{\widetilde{G}} \leq \Omega_{\rm dm}$ [76,69,77,78,74,23]. These $m_{\widetilde{G}}$-dependent limits are shown in Fig. 3 (from [23]) and can be confronted with inflation models. Moreover, $T_{\rm R}$ limits are important for our understanding of the baryon asymmetry and, in particular, for thermal leptogenesis [79,80]. For given $\Omega^{\rm TP}_{\widetilde{G}}$, the bound $\Omega^{\rm NTP}_{\widetilde{G}} \leq \Omega_{\rm dm} - \Omega^{\rm TP}_{\widetilde{G}}$ gives upper limits on $m_{\widetilde{G}}$ and $m_{\widetilde{\tau}_1}$. The limits obtained for a $\widetilde{\tau}_1$ NLSP with (9) are shown in Fig. 4. In Fig. 5 (from [83]) regions with $\Omega_{\widetilde{G}} \in \Omega^{3\sigma}_{\rm dm}$ are shown for $T_{\rm R} = 10^7$, 10^8, and 10^9 GeV. Here both $\Omega^{\rm TP}_{\widetilde{G}}$ and $\Omega^{\rm NTP}_{\widetilde{G}}$ are taken into account for $m_{\widetilde{G}} = m_0$ within the framework of the CMSSM.

While thermally produced gravitinos have a negligible free–streaming velocity today, gravitinos from NLSP decays can be warm/hot dark matter. In the $\widetilde{\tau}_1$ NLSP case, for example, upper limits on the free–streaming velocity from simulations and observations of cosmic structures exclude $m_{\widetilde{\tau}_1} \lesssim 0.7$ TeV for $\Omega^{\rm NTP}_{\widetilde{G}} \simeq \Omega_{\rm dm}$ [74]. Such scenarios (gray band in Fig. 4), however, require $m_{\widetilde{\tau}_1} \gtrsim 0.7$ TeV anyhow and could even resolve the small scale structure problems inherent to cold dark matter [86,87,88].

3.2 Cosmological Constraints

In the $\widetilde{G}$ LSP case with conserved R-parity, the NLSP can have a long lifetime $\tau_{\rm NLSP}$.[10] This is illustrated by the dotted $\tau_{\rm NLSP}$ contours in Figs. 4 and 5. In particular, for the $\widetilde{\tau}_1$ NLSP, one finds in the limit $m_\tau \to 0$,

$$\tau_{\widetilde{\tau}_1} \simeq \Gamma^{-1}(\widetilde{\tau}_1 \to \widetilde{G}\tau) = \frac{48\pi m^2_{\widetilde{G}} \mathrm{M}^2_{\rm P}}{m^5_{\widetilde{\tau}_1}} \left(1 - \frac{m^2_{\widetilde{G}}}{m^2_{\widetilde{\tau}_1}}\right)^{-4}, \tag{10}$$

while the expression for the lifetime of the $\widetilde{\chi}^0_1$ NLSP is given in Sec. IIC of Ref. [71].

If the NLSP decays into the $\widetilde{G}$ LSP occur during or after big-bang nucleosynthesis (BBN), the Standard Model particles emitted in addition to the gravitino can affect the abundances of the primordial light elements. Indeed, these BBN constraints disfavor the $\widetilde{\chi}^0_1$ NLSP for $m_{\widetilde{G}} \gtrsim 100$ MeV [71,77,78,85]. For the slepton NLSP case, the BBN constraints associated with electromagnetic/hadronic energy injection have also been considered and found to be much weaker but still

[10] For the case of broken R-parity, see, e.g., [16,17,18].

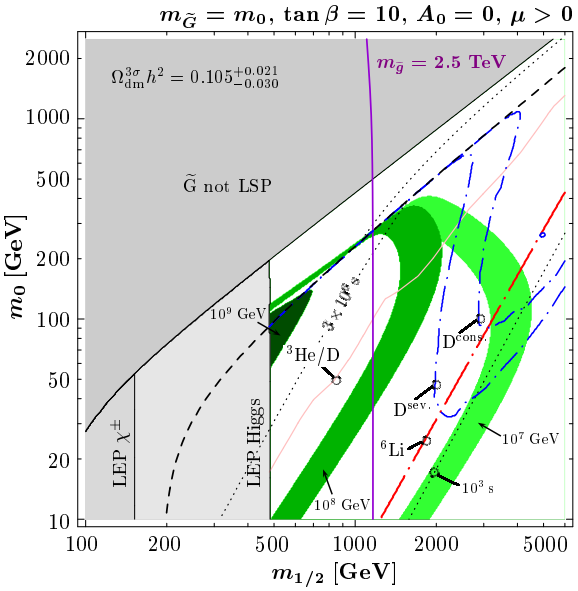

Fig. 5. CMSSM regions with $\Omega_{\widetilde{G}}h^2 \in \Omega^{3\sigma}_{\rm dm}$ for $T_{\rm R} = 10^7$, 10^8, and 10^9 GeV indicated respectively by the light, medium, and dark shaded (green in the web version) bands in the $(m_{1/2}, m_0)$ planes for $\tan\beta = 10$, $A_0 = 0$, $\mu > 0$, and $m_{\widetilde{G}} = m_0$. The regions excluded by the chargino and Higgs mass bounds and the line indicating $m_{\widetilde{\chi}^0_1} = m_{\widetilde{\tau}_1}$ are identical to the ones shown in Fig. 1. In the dark gray region, the gravitino is not the LSP. The dotted lines show contours of the NLSP lifetime. The region to the left of the long-dash-dotted (red in the web version) line and to the left of the thin gray (pink in the web version) line is disfavored by the observationally inferred abundances of primordial ^{6}Li [67] and ^{3}He/D [81]. The effect of hadronic energy injection on primordial D [74] disfavors the $\widetilde{\tau}_1$ NLSP region above the short-dash-dotted (blue in the web version) lines. The $\widetilde{\chi}^0_1$ NLSP region is disfavored by BBN constraints from energy injection [84,71,77,78,85]. On the solid vertical line (violet in the web version) $m_{\tilde{g}} = 2.5$ TeV. From [83].

significant in much of the parameter space [71,77,78,74] as can be seen in Fig. 4, where the constraints from electromagnetic and hadronic energy release are shown respectively by the short-dashed and the short-dash-dotted (blue in the web version) lines. The hadronic constraints are also shown in Fig. 5.

It has been realized only recently that already the mere presence of long-lived negatively charged particles can affect BBN substantially via bound-state effects [89,90,91,85,92,93,94,95,96]. In particular, bound-state formation of $\widetilde{\tau}^-_1$ with ^{4}He can lead to an overproduction of ^{6}Li via the catalyzed BBN (CBBN) reaction $(^4{\rm He}X^-) + {\rm D} \to {}^6{\rm Li} + X^-$ [89]. Thereby, the observationally inferred upper limit on the primordial ^{6}Li abundance $^6{\rm Li/H}|_{\rm obs} \lesssim 2\times10^{-11}$ [82], leads to the CBBN constraint shown by the long-dash-dotted (red in the web version) lines in Figs. 4 and 5, as obtained from [67]. Indeed, for a typical yield (9), the $^6{\rm Li/H}|_{\rm obs}$ limit quoted above implies the constraint [89,92,93,97,67]: $\tau_{\widetilde{\tau}_1} \lesssim 5\times10^3$ s. While numerous other CBBN reactions can affect the abundances of ^{6}Li and other primordial elements significantly [85,93,96,98], the approximate $\tau_{\widetilde{\tau}_1}$ bound is relatively robust. In fact, by systematically taking into account the uncertainties in the relevant nuclear reaction rates, it is shown explicitly in Fig. 14 of [96] and in Fig. 5 of [98] that cosmologically allowed regions for $\tau_{\widetilde{\tau}_1} \gtrsim 10^5$ s are extremely unlikely. In particular, the ^{3}He/D constraint on electromagnetic energy release [99] becomes severe and can exclude $\tau_{\widetilde{\tau}_1} \gtrsim 10^6$ s [78,85,94,96]. This is shown by the long-dashed (green in the web version) line in Fig. 4 and by the thin gray (pink in the web version) line in Fig. 5, which are obtained from Fig. 42 of Ref. [81] for a 'visible' electromagnetic energy of $E_{\rm vis} = \epsilon_{\rm em} = 0.3\,E_\tau$ of the tau energy $E_\tau = (m^2_{\widetilde{\tau}_1} - m^2_{\widetilde{G}} + m^2_\tau)/2m_{\widetilde{\tau}_1}$ released in $\widetilde{\tau}_1 \to \widetilde{G}\tau$.[11]

The observed Planck spectrum of the cosmic microwave background (CMB) provides an additional constraint [100,101] which is not shown. Indeed, the CMB limit derived in [101] is everywhere less severe than the severe electromagnetic limit $D^{\rm sev.}_{\rm em}$ given by the short-dashed (blue in the web version) line in Fig. 4.

As can be seen in Fig. 4, the cosmological constraints provide an upper bound on $m_{\widetilde{G}}$ once $m_{\widetilde{\tau}_1}$ is measured. This bound implies upper bounds on the SUSY breaking scale, $\Omega^{\rm NTP}_{\widetilde{G}}$, and $T_{\rm R}$.

Figure 5 shows that the cosmological constraints imply a lower limit on $m_{1/2}$ [85,23] and an upper limit on $T_{\rm R}$ [23]. Indeed, from $\tau_{\widetilde{\tau}_1} \lesssim 5\times10^3$ s, $m_{\widetilde{G}}$-dependent limits on the gaugino mass parameter,

$$m_{1/2} \geq 0.9\,{\rm TeV}\left(\frac{m_{\widetilde{G}}}{10\ {\rm GeV}}\right)^{2/5}, \qquad (11)$$

and the reheating temperature,

$$T_{\rm R} \leq 4.9\times10^7\ {\rm GeV}\left(\frac{m_{\widetilde{G}}}{10\ {\rm GeV}}\right)^{1/5}, \qquad (12)$$

have been derived within the CMSSM [67].[12] While the $T_{\rm R}$ bound can be restrictive for models of inflation and baryogenesis, the $m_{1/2}$ bound can have implications for SUSY searches at the LHC. Depending on $m_{\widetilde{G}}$, (11) implies sparticle masses which can be associated with a mass range that will be difficult to probe at the LHC. This is illustrated by the vertical (violet in the web version) line in Fig. 5 which indicates the gluino mass $m_{\tilde{g}} = 2.5$ TeV [83].[13]

3.3 Experimental Prospects

Because of its extremely weak couplings, gravitino dark matter is inaccessible to direct and indirect searches if R-parity is conserved.[14] Also the direct production of

[11] With a finely tuned $m_{\widetilde{\tau}_1}$–$m_{\widetilde{G}}$ degeneracy leading to $E_{\rm vis} \to 0$ can any bound on energy release be evaded.

[12] Similar limits have recently been discussed in models where the ratio $m_{\widetilde{G}}/m_{1/2}$ is bounded from below [102].

[13] Note that the mass of the lighter stop is $m_{\widetilde{t}_1} \simeq 0.7 m_{\tilde{g}}$ in the considered $\widetilde{\tau}_1$ NLSP region with $m_{\rm h} > 114.4$ GeV.

[14] For broken R-parity, $\widetilde{G}$ dark matter is unstable so that decay products can appear in indirect searches [17,103,104].

gravitinos at colliders is strongly suppressed. Instead, one expects a large sample of (quasi-) stable NLSPs if the NLSP belongs to the MSSM spectrum.

In the $\widetilde{\tau}_1$ NLSP case, each heavier superpartner produced will cascade down to the $\widetilde{\tau}_1$ which will appear as a (quasi-) stable particle in the detector. Such a heavy charged particle would penetrate the collider detector in a way similar to muons [105,106,107]. If the produced staus are slow, the associated highly ionizing tracks and time–of–flight measurements will allow one to distinguish the $\widetilde{\tau}_1$ from a muon [105,106,107,108]. With measurements of the $\widetilde{\tau}_1$ velocity $\beta_{\tilde{\tau}_1} \equiv v_{\tilde{\tau}_1}/c$ and the slepton momentum $p_{\tilde{\tau}_1} \equiv |\boldsymbol{p}_{\tilde{\tau}_1}|$, $m_{\tilde{\tau}_1}$ can be determined: $m_{\tilde{\tau}_1} = p_{\tilde{\tau}_1}(1-\beta_{\tilde{\tau}_1}^2)^{1/2}/\beta_{\tilde{\tau}_1}$ [108]. For the upcoming LHC experiments, studies of hypothetical scenarios with long-lived charged particles are actively pursued [109,110,111,112]. For example, it has been found that one should be able to measure the mass $m_{\tilde{\tau}_1}$ of a (quasi-) stable $\widetilde{\tau}_1$ quite accurately [109,110].[15]

If some of the staus decay already in the collider detectors, the statistical method proposed in [108] could allow one to measure the $\widetilde{\tau}_1$ lifetime. With (10) and the measured value of $m_{\tilde{\tau}_1}$, one will then be able to determine also the gravitino mass $m_{\widetilde{G}}$ and thereby the scale of SUSY breaking. As a test of our understanding of the early Universe, it will also be interesting to confront the experimentally determined $(m_{\widetilde{G}}, m_{\tilde{\tau}_1})$ point with the cosmological constraints in Fig. 4.

Ways to stop and collect charged long-lived particles for an analysis of their decays have also been proposed [114,115,116,117,118,119]. It was found that up to $\mathcal{O}(10^3$–$10^4)$ and $\mathcal{O}(10^3$–$10^5)$ $\widetilde{\tau}_1$'s can be trapped per year at the LHC and the ILC, respectively, by placing 1–10 kt of massive additional material around planned collider detectors [115,116]. A measurement of $\tau_{\tilde{\tau}_1}$ can then be used to determine $m_{\widetilde{G}}$ as already described above. If $m_{\widetilde{G}}$ can be determined independently from the kinematics of the 2-body decay $\widetilde{\tau}_1 \to \widetilde{G}\tau$,

$$m_{\widetilde{G}} = \sqrt{m_{\tilde{\tau}_1}^2 + m_\tau^2 - 2m_{\tilde{\tau}_1}E_\tau}\,, \tag{13}$$

the lifetime $\tau_{\tilde{\tau}_1}$ can allow for a measurement of the Planck scale [120,121,118,122]

$$\mathrm{M}_{\mathrm{P}}^2 = \frac{\tau_{\tilde{\tau}_1}}{48\pi}\frac{m_{\tilde{\tau}_1}^5}{m_{\widetilde{G}}^2}\left(1-\frac{m_{\widetilde{G}}^2}{m_{\tilde{\tau}_1}^2}\right)^4 . \tag{14}$$

An agreement with (4), which is inferred from Newton's constant [4] $G_{\mathrm{N}} = 6.709\times10^{-39}\,\mathrm{GeV}^{-2}$, would then provide strong evidence for the existence of supergravity in nature [120]. In fact, this agreement would be a striking signature of the gravitino LSP. Unfortunately, the required kinematical determination of $m_{\widetilde{G}}$ appears to be feasible only for [121,118,122] $m_{\widetilde{G}}/m_{\tilde{\tau}_1} \gtrsim 0.1$ which seems to be disfavored according to our present understanding of the cosmological constraints (see Fig. 4).[16] Accordingly, alternative methods such as the ones proposed in [124,125] could become essential to identify the gravitino as the LSP.

[15] (Quasi-) stable $\widetilde{\tau}_1$'s could also be pair-produced in interactions of cosmic neutrinos in the earth matter and be detected in a neutrino telescope such as IceCube [113].

4 Axino Dark Matter

The axino $\widetilde{a}$ [126,127,128,129] appears (as the spin-1/2 superpartner of the axion) once the MSSM is extended with the Peccei–Quinn mechanism [130,131] in order to solve the strong CP problem. Depending on the model and the SUSY breaking scheme, the axino mass $m_{\widetilde{a}}$ can range between the eV and the GeV scale [128,132,133,134,135,136]. The axino is a singlet with respect to the gauge groups of the Standard Model. It interacts extremely weakly since its couplings are suppressed by the Peccei–Quinn scale [4, 137,138,139]

$$f_a \gtrsim 5\times10^9\,\mathrm{GeV} \tag{15}$$

and thus can be classified as an EWIP. The detailed form of the axino interactions depends on the axion model under consideration. We focus on hadronic (or KSVZ) axion models [140,141] in a SUSY setting, in which the axino couples to the MSSM particles only indirectly through loops of additional heavy KSVZ (s)quarks. Considering $\widetilde{a}$ LSP scenarios in which the LOSP is the NLSP, $m_{\tilde{\tau}_1} < m_{\widetilde{\chi}_1^0}$ is again viable.

Before proceeding, it should be stressed that the bosonic partners of the axino, the axion and the saxion, can have important implications for cosmology: (i) The relic density of axions can contribute significantly to the dark matter density [137,138,142] and thereby tighten the constraints from $\Omega_{\widetilde{a}}^{\mathrm{TP}} < \Omega_{\mathrm{dm}}$ discussed below. (ii) Late decays of the saxion can lead to significant entropy production [143,144,145,146] and thereby affect the cosmological constraints [147]. In this review, however, a standard thermal history is assumed which implies that saxion effects are negligible.

4.1 Primordial Origin

Because of their extremely weak interactions, the temperature T_{f} at which axinos decouple from the thermal plasma in the early Universe is very high. For example, an axino decoupling temperature of $T_{\mathrm{f}} \approx 10^9\,\mathrm{GeV}$ is obtained for $f_a = 10^{11}\,\mathrm{GeV}$ [133,148]. For $T_{\mathrm{R}} > T_{\mathrm{f}}$, axinos were in thermal equilibrium before decoupling as a relativistic species so that [133,149,150,148]

$$\Omega_{\widetilde{a}}^{\mathrm{eq}}h^2 \approx \frac{m_{\widetilde{a}}}{2\,\mathrm{keV}}\,. \tag{16}$$

For $T_{\mathrm{R}} < T_{\mathrm{f}}$, axinos are not in thermal equilibrium with the primordial plasma after inflation but can be

[16] Note that the cosmological constraints described in Sect. 3.2 assume a standard thermal history. In fact, entropy production after NLSP decoupling and before BBN can weaken the BBN constraints significantly [123,23].

generated efficiently in scattering processes of particles that are in thermal equilibrium with in the hot SUSY plasma [149,150,148]. Within SUSY QCD, the associated thermally produced (TP) axino density can be calculated in a consistent gauge-invariant treatment that requires weak couplings ($g_{\rm s} \ll 1$) [148]:

$$\Omega_{\widetilde{a}}^{\rm TP} h^2 \simeq 5.5\, g_{\rm s}^6 \ln\left(\frac{1.108}{g_{\rm s}}\right)\left(\frac{10^{11}\,{\rm GeV}}{f_a/N}\right)^2 \times\left(\frac{m_{\widetilde{a}}}{0.1\ {\rm GeV}}\right)\left(\frac{T_R}{10^4\,{\rm GeV}}\right) \qquad (17)$$

with the axion-model-dependent color anomaly N of the Peccei–Quinn symmetry and the strong coupling $g_{\rm s}$ understood to be evaluated at $T_{\rm R}$. The thermally produced axinos do not affect the thermal evolution of the LOSP (or NLSP) which decays after its decoupling into the $\widetilde{a}$ LSP. Taking into account the non-thermally produced (NTP) density from NLSP decays [151,150]

$$\Omega_{\widetilde{a}}^{\rm NTP} h^2 = m_{\widetilde{a}}\, Y_{\rm NLSP}^{\rm dec}\, s(T_0) h^2/\rho_{\rm c}\ , \qquad (18)$$

the guaranteed axino density is[17]

$$\Omega_{\widetilde{a}} = \Omega_{\widetilde{a}}^{\rm eq/TP} + \Omega_{\widetilde{a}}^{\rm NTP}\ . \qquad (19)$$

In Fig. 6 (from [148]) the $(m_{\widetilde{a}}, T_{\rm R})$ region with $0.097 \le \Omega_{\widetilde{a}}^{\rm TP} \le 0.129$ for $f_a/N = 10^{11}\,{\rm GeV}$ is shown by the gray band. Note that (17) shows a different dependence on the LSP mass than the corresponding expression in the $\widetilde{G}$ LSP case (5). Accordingly, one finds the different $m_{\rm LSP}$ dependence of the $T_{\rm R}$ limits inferred from $\Omega_{\widetilde{a}/\widetilde{G}}^{\rm TP} < \Omega_{\rm dm}$. Since thermally produced axinos are generated in kinetic equilibrium with the primordial plasma, they have a thermal spectrum which allows for the $m_{\widetilde{a}}$-dependent classification into cold, warm, and hot dark matter [150] shown in Fig. 6. As can be seen, the $T_{\rm R}$ limit does not exist for $m_{\widetilde{a}} \lesssim 0.2$ keV because of the equality of $\widetilde{a}$ production and $\widetilde{a}$ disappearance rates for $T > T_{\rm f} \approx 10^9$ GeV. With a thermal relic density (16) in this regime, there will be a limit on $m_{\widetilde{a}}$ depending on the constraints inferred from studies of warm/hot dark matter [7].

The non-thermally produced axino density $\Omega_{\widetilde{a}}^{\rm NTP}$ differs from the corresponding expression in the $\widetilde{G}$ LSP case (7) only by the obvious difference in $m_{\widetilde{a}/\widetilde{G}}$. In particular, for given $\Omega_{\widetilde{a}}^{\rm TP}$, the bound $\Omega_{\widetilde{a}}^{\rm NTP} \le \Omega_{\rm dm} - \Omega_{\widetilde{a}}^{\rm eq/TP}$ as obtained with (9) implies limits on $m_{\widetilde{a}}$ and $m_{\widetilde{\tau}_1}$ which can be read off directly from Fig. 4 after the replacement $m_{\widetilde{G}} \to m_{\widetilde{a}}$. Note, however, that the $\tau_{\widetilde{\tau}_1}$ contours and the cosmological constraints are different in the axino LSP case. For the $\widetilde{\tau}_1$ NLSP, the following lifetime was estimated [124]

$$\tau_{\widetilde{\tau}_1} \simeq \Gamma^{-1}(\widetilde{\tau}_1 \to \tau\,\widetilde{a}) \simeq 25\ {\rm s}\ \xi^{-2}\left(1 - \frac{m_{\widetilde{a}}^2}{m_{\widetilde{\tau}_1}^2}\right)^{-1} \times\left(\frac{100\,{\rm GeV}}{m_{\widetilde{\tau}_1}}\right)\left(\frac{f_a/C_{\rm aYY}}{10^{11}\,{\rm GeV}}\right)^2\left(\frac{100\,{\rm GeV}}{m_{\widetilde{B}}}\right)^2, \qquad (20)$$

[17] Axino production in inflaton decays is not considered.

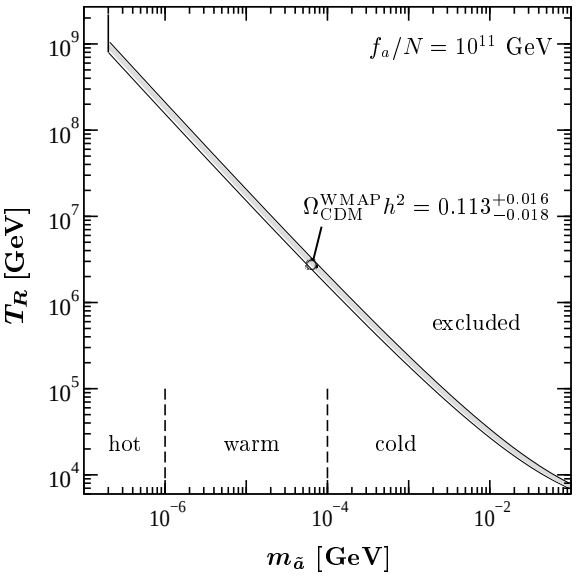

Fig. 6. Upper limits on the reheating temperature $T_{\rm R}$ in the $\widetilde{a}$ LSP case for $f_a/N = 10^{11}$ GeV. On (above) the gray band, $\Omega_{\widetilde{a}}^{\rm TP} h^2 \in 0.113^{+0.016}_{-0.018}$ ($\Omega_{\widetilde{a}}^{\rm TP} h^2 > 0.129$). Thermally produced axinos can be classified as hot, warm, and cold dark matter [150] as indicated. From [148].

where the KSVZ-model dependence is expressed by $C_{\rm aYY} \simeq \mathcal{O}(1)$ and the uncertainty of the estimate is absorbed into $\xi \simeq \mathcal{O}(1)$. One thus finds a $\widetilde{\tau}_1$ lifetime in the $\widetilde{a}$ LSP case that cannot be as large as the one in the $\widetilde{G}$ LSP case (10). Accordingly, the BBN constraints are much weaker for the $\widetilde{a}$ LSP. For discussions of $\widetilde{a}$ LSP scenarios with the $\widetilde{\chi}_1^0$ NLSP, see [151,150,152]. For both the $\widetilde{\tau}_1$ NLSP and the $\widetilde{\chi}_1^0$ NLSP, it has been shown that non-thermally produced axinos with $m_{\widetilde{a}} \lesssim 10$ GeV would be warm/hot dark matter [88].

4.2 Experimental Prospects

Being an EWIP, the axino LSP is inaccessible to any direct and indirect dark matter searches if R-parity is conserved. Also the direct $\widetilde{a}$ production at colliders is strongly suppressed. Nevertheless, (quasi-) stable $\widetilde{\tau}_1$'s could appear in collider detectors (and neutrino telescopes [113]) as a possible signature of the $\widetilde{a}$ LSP. However, since the $M_{\rm P}$ measurement at colliders [120], which would have been a decisive test of the $\widetilde{G}$ LSP, seems cosmologically disfavored, it will be a challenge to distinguish between the $\widetilde{a}$ LSP and the $\widetilde{G}$ LSP.

For $m_{\widetilde{\tau}_1} = 100\,{\rm GeV}$ and $m_{\widetilde{B}} = 110\,{\rm GeV}$, for example, the $\widetilde{\tau}_1$ lifetime in the $\widetilde{a}$ LSP scenario (20) can range from $\mathcal{O}(0.01\ {\rm s})$ for $f_a = 5\times10^9\,{\rm GeV}$ to $\mathcal{O}(10\ {\rm h})$ for $f_a = 5\times10^{12}\,{\rm GeV}$. In the $\widetilde{G}$ LSP case, the corresponding lifetime (10) can vary over an even wider range, e.g., from 6×10^{-8} s for $m_{\widetilde{G}} = 1$ keV to 15 years for $m_{\widetilde{G}} = 50$ GeV. Thus, both a very short lifetime, $\tau_{\widetilde{\tau}_1} \lesssim$ ms, and a very long one, $\tau_{\widetilde{\tau}_1} \gtrsim$ days, will point to the $\widetilde{G}$ LSP. On the other hand, if the LSP mass cannot be measured kinematically and if $\tau_{\widetilde{\tau}_1} = \mathcal{O}(0.01\ {\rm s})$–

$\mathcal{O}(10\text{ h})$, the stau lifetime alone will not allow us to distinguish between the $\widetilde{a}$ LSP and the $\widetilde{G}$ LSP.

The situation is considerably improved when one considers the 3-body decays $\widetilde{\tau}_1 \to \tau\gamma\widetilde{a}/\widetilde{G}$. From the corresponding differential rates [124], one obtains the differential distributions of the visible decay products. These are illustrated in Fig. 7 (from [124]) in terms of

$$\frac{1}{\Gamma(\widetilde{\tau}_1 \to \tau\,\gamma\,i\,;x_\gamma^{\rm cut},x_\theta^{\rm cut})}\,\frac{d^2\Gamma(\widetilde{\tau}_1 \to \tau\,\gamma\,i)}{dx_\gamma d\cos\theta} \qquad (21)$$

where $x_\gamma \equiv 2E_\gamma/m_{\widetilde{\tau}_1}$ is the scaled photon energy, θ the opening angle between the directions of γ and τ,

$$\Gamma(\widetilde{\tau}_1 \to \tau\,\gamma\,i\,;x_\gamma^{\rm cut},x_\theta^{\rm cut}) \equiv \int_{x_\gamma^{\rm cut}}^{1-A_i} dx_\gamma \int_{-1}^{1-x_\theta^{\rm cut}} d\cos\theta \times\frac{d^2\Gamma(\widetilde{\tau}_1 \to \tau\,\gamma\,i)}{dx_\gamma d\cos\theta} \qquad (22)$$

the respective integrated 3-body decay rate with the cuts $x_\gamma > x_\gamma^{\rm cut}$ and $\cos\theta < 1-x_\theta^{\rm cut}$, and $A_i \equiv m_i^2/m_{\widetilde{\tau}_1}^2$. Note that (21) is independent of the 2-body decay, the total NLSP decay rate, and the Peccei–Quinn/Planck scale. The figure shows (21) for the axino LSP ($i=\widetilde{a}$) with $m_{\widetilde{a}}^2/m_{\widetilde{\tau}_1}^2 \ll 1$ (upper panel) and the gravitino LSP ($i=\widetilde{G}$) with $m_{\widetilde{G}} = 10$ MeV (lower panel), where $m_{\widetilde{\tau}_1} = 100$ GeV, $m_{\widetilde{B}} = 110$ GeV, and $x_\gamma^{\rm cut} = x_\theta^{\rm cut} = 0.1$. In the $\widetilde{G}$ LSP case, the events are peaked only in the region where photons are soft and emitted with a small opening angle with respect to the tau ($\theta \simeq 0$). In contrast, in the $\widetilde{a}$ LSP case, the events are also peaked in the region where the photon energy is large and the photon and the tau are emitted back-to-back ($\theta \simeq \pi$). Thus, if the observed number of events peaks in both regions, this can be evidence against the gravitino LSP and a hint towards the axino LSP [124].[18]

To be specific, with 10^4 analyzed stau NLSP decays, we expect about 165±13 (stat.) events for the $\widetilde{a}$ LSP and about 100±10 (stat.) events for the $\widetilde{G}$ LSP [124], which will be distributed over the corresponding $(x_\gamma, \cos\theta)$-planes shown in Fig. 7. In particular, in the region of $x_\gamma \gtrsim 0.8$ and $\cos\theta \lesssim -0.3$, we expect about 28% of the 165±13 (stat.) events in the $\widetilde{a}$ LSP case and about 1% of the 100±10 (stat.) events in the $\widetilde{G}$ LSP case. These numbers illustrate that $\mathcal{O}(10^4)$ of analyzed stau NLSP decays could be sufficient for the distinction based on the differential distributions. To establish the feasibility of this distinction, dedicated studies including details of the detectors and the additional massive material will be crucial [118].

4.3 Probing the Peccei-Quinn Scale f_a and $m_{\widetilde{a}}$

If $\widetilde{a}$ is the LSP and $\widetilde{\tau}_1$ the NLSP, the analysis of the 2-body decay $\widetilde{\tau}_1 \to \tau\widetilde{a}$ will allow us to probe the Peccei-Quinn scale f_a and the axino mass $m_{\widetilde{a}}$. In fact, the measurement of $\tau_{\widetilde{\tau}_1}$ (20) with methods described in Sect. 3.3 leads to the following estimate of the Peccei-Quinn scale f_a [124]:

$$f_a^2 \simeq \xi^2\, C_{\rm aYY}^2 \left(10^{11}\,\text{GeV}\right)^2 \left(1-\frac{m_{\widetilde{a}}^2}{m_{\widetilde{\tau}_1}^2}\right)\left(\frac{\tau_{\widetilde{\tau}_1}}{25\text{ s}}\right) \times\left(\frac{m_{\widetilde{\tau}_1}}{100\,\text{GeV}}\right)\left(\frac{m_{\widetilde{B}}}{100\,\text{GeV}}\right)^2 , \qquad (23)$$

which can be confronted with f_a limits from astrophysical axion studies and axion searches in the laboratory [4,137,138,139,153]. Indeed, we expect that $m_{\widetilde{\tau}_1}$ and $m_{\widetilde{B}}$ will already be known from other processes when the $\widetilde{\tau}_1$ NLSP decays are analyzed; cf. Sect. 3.3. The dependence on $m_{\widetilde{a}}$ is negligible for $m_{\widetilde{a}}/m_{\widetilde{\tau}_1} \lesssim 0.1$.

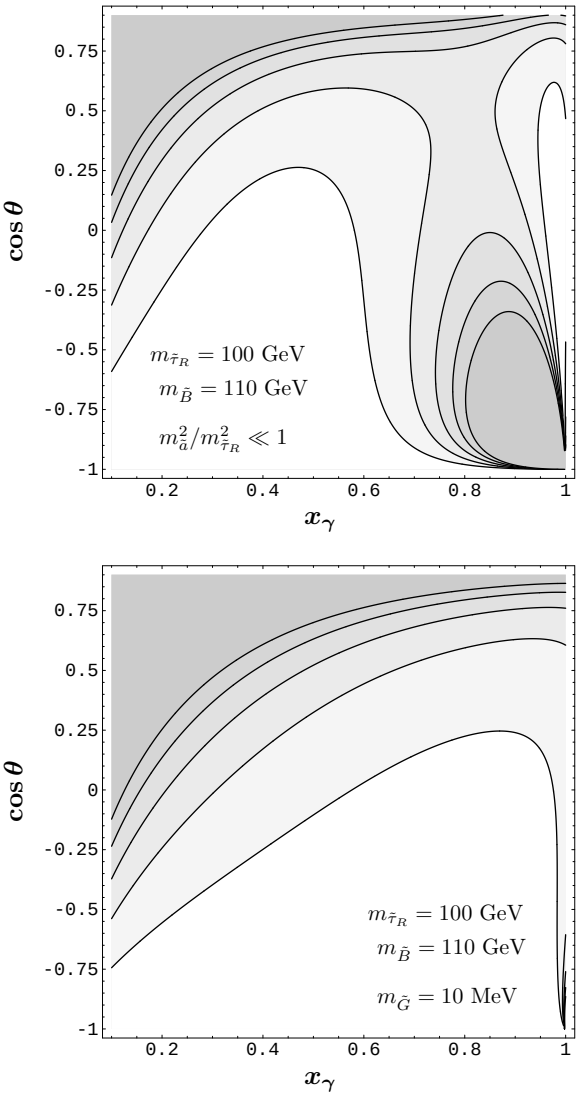

Fig. 7. The normalized differential distributions (21) of the visible decay products in the decays $\widetilde{\tau}_1 \to \tau + \gamma + \widetilde{a}/\widetilde{G}$ for the cases of the $\widetilde{a}$ LSP (upper panel) and the $\widetilde{G}$ LSP (lower panel) for $m_{\widetilde{\tau}_1} = 100\,\text{GeV}$, $\widetilde{\chi}_1^0 \simeq \widetilde{B}$, $m_{\widetilde{B}} = 110\,\text{GeV}$, $m_{\widetilde{a}}^2/m_{\widetilde{\tau}_1}^2 \ll 1$, and $m_{\widetilde{G}} = 10\,\text{MeV}$. The cut parameters are set to $x_\gamma^{\rm cut} = x_\theta^{\rm cut} = 0.1$. The contour lines represent the values 0.2, 0.4, 0.6, 0.8, and 1.0, where the darker shading implies a higher number of events. From [124].

[18] There is a caveat: If $m_{\widetilde{G}} < m_{\widetilde{a}} < m_{\widetilde{\tau}_1}$ and $\Gamma(\widetilde{\tau}_1 \to \widetilde{a}\,X) \gg \Gamma(\widetilde{\tau}_1 \to \widetilde{G}\,X)$, one would still find the distribution shown in the upper panel of Fig. 7. The axino would then eventually decay into the gravitino LSP and the axion.

For larger values of $m_{\widetilde{a}}$, the $\widetilde{\tau}_1$ NLSP decays can be used to determine $m_{\widetilde{a}}$ from the kinematics of the 2-body decay, i.e., from a measurement of the energy of the emitted tau E_τ,

$$m_{\widetilde{a}} = \sqrt{m_{\widetilde{\tau}_1}^2 + m_\tau^2 - 2m_{\widetilde{\tau}_1} E_\tau} \ , \qquad (24)$$

with an error governed by the experimental uncertainties on $m_{\widetilde{\tau}_1}$ and E_τ. As is evident from (17) and (18), the determination of both the Peccei–Quinn scale f_a and the axino mass $m_{\widetilde{a}}$ is crucial for insights into the cosmological relevance of the axino LSP.

5 Conclusion

Dark matter is strong evidence for physics beyond the Standard Model. Extending the Standard Model with SUSY, an electrically neutral and color neutral LSP becomes a dark matter candidate for conserved R-parity. I have shown that the neutralino $\widetilde{\chi}_1^0$, the gravitino $\widetilde{G}$, and the axino $\widetilde{a}$ can be the LSP and as such explain the non-baryonic dark matter in our Universe. The neutralino $\widetilde{\chi}_1^0$ is already part of the MSSM which provides a solution of the hierarchy problem and allows for gauge coupling unification. Being the superpartner of the graviton and the gauge field associated with supergravity, the gravitino $\widetilde{G}$ is equally well motivated with a mass $m_{\widetilde{G}}$ that reflects the SUSY breaking scale. As the superpartner of the axion, also the axino $\widetilde{a}$ appears naturally once the strong CP problem is solved with the Peccei–Quinn mechanism in a SUSY setting.

While mass values and interactions can be very different for the $\widetilde{\chi}_1^0$, $\widetilde{G}$, and $\widetilde{a}$, I have illustrated for each of these LSP candidates that natural regions in the parameter space exist in which $\Omega_{\rm LSP} = \Omega_{\rm dm}$. These regions are limited by bounds from electroweak precision observables, B-physics observables, Higgs and sparticle searches at LEP, and by BBN constraints. The constraints from $\Omega_{\rm dm}$ and BBN also imply serious upper limits on the reheating temperature after inflation $T_{\rm R}$ which can be relevant for models of inflation and baryogenesis.

Most promising are the experimental prospects in the case of the $\widetilde{\chi}_1^0$ LSP. Being a WIMP, the $\widetilde{\chi}_1^0$ LSP should be accessible in direct and indirect dark matter searches. Indeed, first hints might have already been found in the EGRET data [33,34]. With ongoing indirect searches, the increasing sensitivity of direct searches, and the advent of the LHC at which $\widetilde{\chi}_1^0$ dark matter could be produced, we will be able to test whether these hints are indeed the first evidence for the existence of SUSY dark matter. While an excess in missing transverse energy is expected to be the first evidence for SUSY at the LHC already within the next three years, the identification of the $\widetilde{\chi}_1^0$ being the LSP will require the reconstruction of the SUSY model realized in nature. If superparticles are within the kinematical reach, precision studies at the ILC will be crucial for this endeavor.

In the $\widetilde{G}/\widetilde{a}$ LSP scenarios with conserved R-parity, no dark matter signal should appear in direct or indirect searches. However, since an electrically charged LOSP such as the $\widetilde{\tau}_1$ is viable in the $\widetilde{G}/\widetilde{a}$ LSP scenarios, (quasi-) stable $\widetilde{\tau}_1$'s might occur as muon-like particles instead of an excess in missing transverse energy. Indeed, an excess of (quasi-) stable $\widetilde{\tau}_1$'s could appear as an alternative first evidence for SUSY at the LHC in the next three years. Because of the severe upper limits on the abundance of stable charged particles [4], one would then expect that the $\widetilde{\tau}_1$ is the NLSP that decays eventually into the $\widetilde{G}/\widetilde{a}$ LSP or that R-parity is broken. A distinction between these scenarios will require the analysis of the $\widetilde{\tau}_1$ decays. For this challenge, the ILC with its tunable beam energy seems crucial [115, 116,121,118,122].

Table 2 presents an overview of the SUSY dark matter candidates discussed in this review. As the LSP, each of them—the lightest neutralino $\widetilde{\chi}_1^0$, the gravitino $\widetilde{G}$, or the axino $\widetilde{a}$—could provide $\Omega_{\rm dm}$ and could be produced and identified at colliders in the near future.

I would like to thank the organizers of SUSY 2007 for inviting me to an exciting and stimulating conference. I am grateful to A. Brandenburg, L. Covi, A. Freitas, K. Hamaguchi, G. Panotopoulos, T. Plehn, J. Pradler, L. Roszkowski, S. Schilling, N. Tajuddin, Y. Y. Y. Wong, D. Wyler, and M. Zagermann for valuable discussions and collaborations on the topics covered in this review.

References

1. L. Bergstrom, Rept. Prog. Phys. **63**, 793 (2000), `hep-ph/0002126`
2. G. Bertone, D. Hooper, J. Silk, Phys. Rept. **405**, 279 (2005), `hep-ph/0404175`
3. D.N. Spergel et al. (WMAP), Astrophys. J. Suppl. **170**, 377 (2007), `astro-ph/0603449`
4. W.M. Yao et al. (Particle Data Group), J. Phys. **G33**, 1 (2006)
5. J. Hamann, S. Hannestad, M.S. Sloth, Y.Y.Y. Wong, Phys. Rev. **D75**, 023522 (2007), `astro-ph/0611582`
6. J. Lesgourgues, S. Pastor, Phys. Rept. **429**, 307 (2006), `astro-ph/0603494`
7. S. Hannestad, A. Mirizzi, G.G. Raffelt, Y.Y.Y. Wong, JCAP **0708**, 015 (2007), `arXiv:0706.4198 [astro-ph]`
8. J. Wess, J. Bagger, *Supersymmetry and supergravity*, Princeton University Press, Princeton, USA (1992) 259 p
9. H.P. Nilles, Phys. Rept. **110**, 1 (1984)
10. H.E. Haber, G.L. Kane, Phys. Rept. **117**, 75 (1985)
11. S.P. Martin (1997), `hep-ph/9709356`
12. M. Drees, R. Godbole, P. Roy, *Sparticles*, World Scientific, Hackensack, USA, (2004) 555 p
13. H. Baer, X. Tata , *Weak Scale Supersymmetry*, Cambridge University Press, Cambridge, UK (2006) 537 p
14. H.K. Dreiner (1997), `hep-ph/9707435`
15. B.C. Allanach et al. (2007), `arXiv:0710.2034 [hep-ph]`

Table 2. Supersymmetric dark matter candidates, their identity, and key properties. With the listed production mechanisms, $\Omega_{\rm LSP} = \Omega_{\rm dm}$ is possible. The respective production leads typically to a cold, warm, or hot dark matter component as indicated. Quantities marked with '(?)' seem to be unaccessible in light of the current understanding of cosmological constraints within a standard thermal history.

LSP	identity	mass	interactions	production	constraints	experiments
$\widetilde{\chi}_1^0$	lightest neutralino (spin 1/2) mixture of $\widetilde{B}$, $\widetilde{W}$, $\widetilde{H}_u^0$, $\widetilde{H}_d^0$	$\mathcal{O}(100\,\mathrm{GeV})$	g, g', y_i weak $M_{\rm W} \sim 100$ GeV	therm. relic	$\leftarrow$ cold	indirect searches direct searches collider searches
$\widetilde{G}$	gravitino (spin 3/2) superpartner of the graviton	eV–TeV	$(p/\mathrm{M_P})^n$ extremely weak $\mathrm{M_P} = 2.4\times10^{18}$ GeV	therm. prod. NLSP decay	$\leftarrow$ cold $\leftarrow$ warm BBN	$\widetilde{\tau}_1$ prod. at colliders $+\ \widetilde{\tau}_1$ collection $+\ \widetilde{\tau}_1$ decay analysis $\hookrightarrow m_{\widetilde{G}}$, $\mathrm{M_P}$ (?)
$\widetilde{a}$	axino (spin 1/2) superpartner of the axion	eV–GeV	$(p/f_a)^n$ extremely weak $f_a \gtrsim 10^9$ GeV	therm. relic. therm. prod. NLSP decay	$\leftarrow$ hot/warm $\leftarrow$ cold/warm $\leftarrow$ warm/hot BBN	$\widetilde{\tau}_1$ prod. at colliders $+\ \widetilde{\tau}_1$ collection $+\ \widetilde{\tau}_1$ decay analysis $\hookrightarrow m_{\widetilde{a}}$ (?), f_a

16. F. Takayama, M. Yamaguchi, Phys. Lett. **B485**, 388 (2000), hep-ph/0005214
17. W. Buchmüller, L. Covi, K. Hamaguchi, A. Ibarra, T. Yanagida, JHEP **03**, 037 (2007), hep-ph/0702184
18. A. Ibarra (2007), arXiv:0710.2287 [hep-ph]
19. G. Jungman, M. Kamionkowski, K. Griest, Phys. Rept. **267**, 195 (1996), hep-ph/9506380
20. K.A. Olive (2007), arXiv:0709.3303 [hep-ph]
21. G. Bertone (2007), arXiv:0710.5603 [astro-ph]
22. A. Brignole, L.E. Ibanez, C. Munoz (1997), hep-ph/9707209
23. J. Pradler, F.D. Steffen, Phys. Lett. **B648**, 224 (2007), hep-ph/0612291
24. A. Djouadi, J.L. Kneur, G. Moultaka, Comput. Phys. Commun. **176**, 426 (2007), hep-ph/0211331
25. G. Belanger, F. Boudjema, A. Pukhov, A. Semenov, Comput. Phys. Commun. **149**, 103 (2002), hep-ph/0112278
26. G. Belanger, F. Boudjema, A. Pukhov, A. Semenov, Comput. Phys. Commun. **174**, 577 (2006), hep-ph/0405253
27. P. Gondolo et al., JCAP **0407**, 008 (2004), astro-ph/0406204
28. A. Djouadi, M. Drees, J.L. Kneur, JHEP **03**, 033 (2006), hep-ph/0602001
29. R. Lafaye, T. Plehn, D. Zerwas (2004), hep-ph/0404282
30. P. Bechtle, K. Desch, P. Wienemann, Comput. Phys. Commun. **174**, 47 (2006), hep-ph/0412012
31. E.A. Baltz, M. Battaglia, M.E. Peskin, T. Wizansky, Phys. Rev. **D74**, 103521 (2006), hep-ph/0602187
32. L. Baudis (2007), arXiv:0711.3788 [astro-ph]
33. W. de Boer, C. Sander, V. Zhukov, A.V. Gladyshev, D.I. Kazakov, Phys. Lett. **B636**, 13 (2006), hep-ph/0511154
34. D. Elsaesser, K. Mannheim, Phys. Rev. Lett. **94**, 171302 (2005), astro-ph/0405235
35. D. Hooper (2007), arXiv:0710.2062 [hep-ph]
36. G. Angloher et al. (CRESST), Astropart. Phys. **23**, 325 (2005), astro-ph/0408006
37. V. Sanglard et al. (EDELWEISS), Phys. Rev. **D71**, 122002 (2005), astro-ph/0503265
38. D.S. Akerib et al. (CDMS), Phys. Rev. Lett. **96**, 011302 (2006), astro-ph/0509259
39. J. Angle et al. (XENON) (2007), arXiv:0706.0039 [astro-ph]
40. M. Drees, C.L. Shan, JCAP **0706**, 011 (2007), astro-ph/0703651
41. C.L. Shan, M. Drees (2007), arXiv:0710.4296 [hep-ph]
42. A. Duperrin (CDF) (2007), arXiv:0710.4265 [hep-ex]
43. M. Shamim (D0) (2007), arXiv:0710.2897 [hep-ex]
44. M. Tytgat (2007), arXiv:0710.1013 [hep-ex]
45. S. Yamamoto (ATLAS) (2007), arXiv:0710.3953 [hep-ex]
46. N. Ozturk (ATLAS) (2007), arXiv:0710.4546 [hep-ph]
47. G. Weiglein et al. (LHC/LC Study Group), Phys. Rept. **426**, 47 (2006), hep-ph/0410364
48. S.Y. Choi (2007), arXiv:0711.1393 [hep-ph]
49. S.Y. Choi, K. Hagiwara, H.U. Martyn, K. Mawatari, P.M. Zerwas, Eur. Phys. J. **C51**, 753 (2007), hep-ph/0612301
50. M. Dine, A.E. Nelson, Y. Shirman, Phys. Rev. **D51**, 1362 (1995), hep-ph/9408384
51. M. Dine, A.E. Nelson, Y. Nir, Y. Shirman, Phys. Rev. **D53**, 2658 (1996), hep-ph/9507378
52. G.F. Giudice, R. Rattazzi, Phys. Rept. **322**, 419 (1999), hep-ph/9801271
53. L. Randall, R. Sundrum, Nucl. Phys. **B557**, 79 (1999), hep-th/9810155
54. G.F. Giudice, M.A. Luty, H. Murayama, R. Rattazzi, JHEP **12**, 027 (1998), hep-ph/9810442
55. W. Buchmüller, K. Hamaguchi, J. Kersten, Phys. Lett. **B632**, 366 (2006), hep-ph/0506105
56. E. Cremmer, S. Ferrara, L. Girardello, A. Van Proeyen, Nucl. Phys. **B212**, 413 (1983)
57. J.L. Diaz-Cruz, J.R. Ellis, K.A. Olive, Y. Santoso, JHEP **05**, 003 (2007), hep-ph/0701229

58. E.A. Baltz, H. Murayama, JHEP **05**, 067 (2003), astro-ph/0108172
59. M. Fujii, T. Yanagida, Phys. Lett. **B549**, 273 (2002), hep-ph/0208191
60. M. Fujii, M. Ibe, T. Yanagida, Phys. Rev. **D69**, 015006 (2004), hep-ph/0309064
61. M. Lemoine, G. Moultaka, K. Jedamzik, Phys. Lett. **B645**, 222 (2007), hep-ph/0504021
62. K. Jedamzik, M. Lemoine, G. Moultaka, Phys. Rev. **D73**, 043514 (2006), hep-ph/0506129
63. G. Moultaka (2007), arXiv:0710.5121 [hep-ph]
64. M. Bolz, A. Brandenburg, W. Buchmüller, Nucl. Phys. **B606**, 518 (2001), hep-ph/0012052
65. J. Pradler, F.D. Steffen, Phys. Rev. **D75**, 023509 (2007), hep-ph/0608344
66. V.S. Rychkov, A. Strumia, Phys. Rev. **D75**, 075011 (2007), hep-ph/0701104
67. J. Pradler, F.D. Steffen (2007), arXiv:0710.2213 [hep-ph]
68. S. Borgani, A. Masiero, M. Yamaguchi, Phys. Lett. **B386**, 189 (1996), hep-ph/9605222
69. T. Asaka, K. Hamaguchi, K. Suzuki, Phys. Lett. **B490**, 136 (2000), hep-ph/0005136
70. J.L. Feng, A. Rajaraman, F. Takayama, Phys. Rev. Lett. **91**, 011302 (2003), hep-ph/0302215
71. J.L. Feng, S. Su, F. Takayama, Phys. Rev. **D70**, 075019 (2004), hep-ph/0404231
72. T. Asaka, S. Nakamura, M. Yamaguchi, Phys. Rev. **D74**, 023520 (2006), hep-ph/0604132
73. M. Endo, F. Takahashi, T.T. Yanagida, Phys. Rev. **D76**, 083509 (2007), arXiv:0706.0986 [hep-ph]
74. F.D. Steffen, JCAP **0609**, 001 (2006), hep-ph/0605306
75. F.D. Steffen, AIP Conf. Proc. **903**, 595 (2007), hep-ph/0611027
76. T. Moroi, H. Murayama, M. Yamaguchi, Phys. Lett. **B303**, 289 (1993)
77. L. Roszkowski, R. Ruiz de Austri, K.Y. Choi, JHEP **08**, 080 (2005), hep-ph/0408227
78. D.G. Cerdeno, K.Y. Choi, K. Jedamzik, L. Roszkowski, R. Ruiz de Austri, JCAP **0606**, 005 (2006), hep-ph/0509275
79. M. Fukugita, T. Yanagida, Phys. Lett. **B174**, 45 (1986), hep-ph/0208191
80. W. Buchmüller, P. Di Bari, M. Plümacher, Ann. Phys. **315**, 305 (2005), hep-ph/0401240
81. M. Kawasaki, K. Kohri, T. Moroi, Phys. Rev. **D71**, 083502 (2005), astro-ph/0408426
82. R.H. Cyburt, J.R. Ellis, B.D. Fields, K.A. Olive, Phys. Rev. **D67**, 103521 (2003), astro-ph/0211258
83. J. Pradler, F.D. Steffen (2007), arXiv:0710.4548 [hep-ph]
84. J.R. Ellis, K.A. Olive, Y. Santoso, V.C. Spanos, Phys. Lett. **B588**, 7 (2004), hep-ph/0312262
85. R.H. Cyburt, J.R. Ellis, B.D. Fields, K.A. Olive, V.C. Spanos, JCAP **0611**, 014 (2006), astro-ph/0608562
86. J.A.R. Cembranos, J.L. Feng, A. Rajaraman, F. Takayama, Phys. Rev. Lett. **95**, 181301 (2005), hep-ph/0507150
87. M. Kaplinghat, Phys. Rev. **D72**, 063510 (2005), astro-ph/0507300
88. K. Jedamzik, M. Lemoine, G. Moultaka, JCAP **0607**, 010 (2006), astro-ph/0508141
89. M. Pospelov, Phys. Rev. Lett. **98**, 231301 (2007), hep-ph/0605215
90. K. Kohri, F. Takayama, Phys. Rev. **D76**, 063507 (2007), hep-ph/0605243
91. M. Kaplinghat, A. Rajaraman, Phys. Rev. **D74**, 103004 (2006), astro-ph/0606209
92. K. Hamaguchi, T. Hatsuda, M. Kamimura, Y. Kino, T.T. Yanagida, Phys. Lett. **B650**, 268 (2007), hep-ph/0702274
93. C. Bird, K. Koopmans, M. Pospelov (2007), hep-ph/0703096
94. M. Kawasaki, K. Kohri, T. Moroi, Phys. Lett. **B649**, 436 (2007), hep-ph/0703122
95. T. Jittoh et al. (2007), arXiv:0704.2914 [hep-ph]
96. K. Jedamzik (2007), arXiv:0707.2070v3 [astro-ph]
97. F. Takayama (2007), arXiv:0704.2785 [hep-ph]
98. K. Jedamzik (2007), arXiv:0710.5153 [hep-ph]
99. G. Sigl, K. Jedamzik, D.N. Schramm, V.S. Berezinsky, Phys. Rev. **D52**, 6682 (1995), astro-ph/9503094
100. W. Hu, J. Silk, Phys. Rev. **D48**, 485 (1993)
101. R. Lamon, R. Durrer, Phys. Rev. **D73**, 023507 (2006), hep-ph/0506229
102. J. Kersten, K. Schmidt-Hoberg (2007), arXiv:0710.4528 [hep-ph]
103. G. Bertone, W. Buchmüller, L. Covi, A. Ibarra (2007), arXiv:0709.2299 [astro-ph]
104. A. Ibarra, D. Tran (2007), arXiv:0709.4593 [astro-ph]
105. M. Drees, X. Tata, Phys. Lett. **B252**, 695 (1990)
106. A. Nisati, S. Petrarca, G. Salvini, Mod. Phys. Lett. **A12**, 2213 (1997), hep-ph/9707376
107. J.L. Feng, T. Moroi, Phys. Rev. **D58**, 035001 (1998), hep-ph/9712499
108. S. Ambrosanio, B. Mele, S. Petrarca, G. Polesello, A. Rimoldi, JHEP **01**, 014 (2001), hep-ph/0010081
109. J.R. Ellis, A.R. Raklev, O.K. Oye, JHEP **10**, 061 (2006), hep-ph/0607261
110. J. Ellis (2007), arXiv:0710.4959 [hep-ph]
111. S. Bressler (ATLAS) (2007), arXiv:0710.2111 [hep-ex]
112. P. Zalewski (2007), arXiv:0710.2647 [hep-ph]
113. M. Ahlers, J. Kersten, A. Ringwald, JCAP **0607**, 005 (2006), hep-ph/0604188
114. J.L. Goity, W.J. Kossler, M. Sher, Phys. Rev. **D48**, 5437 (1993), hep-ph/9305244
115. K. Hamaguchi, Y. Kuno, T. Nakaya, M.M. Nojiri, Phys. Rev. **D70**, 115007 (2004), hep-ph/0409248
116. J.L. Feng, B.T. Smith, Phys. Rev. **D71**, 015004 (2005), hep-ph/0409278
117. A. De Roeck et al., Eur. Phys. J. **C49**, 1041 (2007), hep-ph/0508198
118. K. Hamaguchi, M.M. Nojiri, A. de Roeck, JHEP **03**, 046 (2007), hep-ph/0612060
119. O. Cakir, I.T. Cakir, J.R. Ellis, Z. Kirca (2007), hep-ph/0703121
120. W. Buchmüller, K. Hamaguchi, M. Ratz, T. Yanagida, Phys. Lett. **B588**, 90 (2004), hep-ph/0402179
121. H.U. Martyn, Eur. Phys. J. **C48**, 15 (2006), hep-ph/0605257
122. H.U. Martyn (2007), arXiv:0709.1030 [hep-ph]
123. W. Buchmüller, K. Hamaguchi, M. Ibe, T.T. Yanagida, Phys. Lett. **B643**, 124 (2006), hep-ph/0605164
124. A. Brandenburg, L. Covi, K. Hamaguchi, L. Roszkowski, F.D. Steffen, Phys. Lett. **B617**, 99 (2005), hep-ph/0501287

125. F.D. Steffen (2005), hep-ph/0507003
126. H.P. Nilles, S. Raby, Nucl. Phys. **B198**, 102 (1982)
127. J.E. Kim, H.P. Nilles, Phys. Lett. **B138**, 150 (1984)
128. K. Tamvakis, D. Wyler, Phys. Lett. **B112**, 451 (1982)
129. J.E. Kim, Phys. Lett. **B136**, 378 (1984)
130. R.D. Peccei, H.R. Quinn, Phys. Rev. Lett. **38**, 1440 (1977)
131. R.D. Peccei, H.R. Quinn, Phys. Rev. **D16**, 1791 (1977)
132. J.F. Nieves, Phys. Rev. **D33**, 1762 (1986)
133. K. Rajagopal, M.S. Turner, F. Wilczek, Nucl. Phys. **B358**, 447 (1991)
134. T. Goto, M. Yamaguchi, Phys. Lett. **B276**, 103 (1992)
135. E.J. Chun, J.E. Kim, H.P. Nilles, Phys. Lett. **B287**, 123 (1992), hep-ph/9205229
136. E.J. Chun, A. Lukas, Phys. Lett. **B357**, 43 (1995), hep-ph/9503233
137. P. Sikivie (2006), astro-ph/0610440
138. G.G. Raffelt, J. Phys. **A40**, 6607 (2007), hep-ph/0611118
139. G.G. Raffelt (2006), hep-ph/0611350
140. J.E. Kim, Phys. Rev. Lett. **43**, 103 (1979)
141. M.A. Shifman, A.I. Vainshtein, V.I. Zakharov, Nucl. Phys. **B166**, 493 (1980)
142. F. Wilczek (2007), arXiv:0708.4236 [hep-ph]
143. J.E. Kim, Phys. Rev. Lett. **67**, 3465 (1991)
144. D.H. Lyth, Phys. Rev. **D48**, 4523 (1993), hep-ph/9306293
145. S. Chang, H.B. Kim, Phys. Rev. Lett. **77**, 591 (1996), hep-ph/9604222
146. M. Hashimoto, K.I. Izawa, M. Yamaguchi, T. Yanagida, Phys. Lett. **B437**, 44 (1998), hep-ph/9803263
147. M. Kawasaki, K. Nakayama, M. Senami (2007), arXiv:0711.3083 [hep-ph]
148. A. Brandenburg, F.D. Steffen, JCAP **0408**, 008 (2004), hep-ph/0405158; hep-ph/0406021; hep-ph/0407324
149. T. Asaka, T. Yanagida, Phys. Lett. **B494**, 297 (2000), hep-ph/0006211
150. L. Covi, H.B. Kim, J.E. Kim, L. Roszkowski, JHEP **05**, 033 (2001), hep-ph/0101009
151. L. Covi, J.E. Kim, L. Roszkowski, Phys. Rev. Lett. **82**, 4180 (1999), hep-ph/9905212
152. L. Covi, L. Roszkowski, R. Ruiz de Austri, M. Small, JHEP **06**, 003 (2004), hep-ph/0402240
153. A. Ringwald, Phys. Lett. **B569**, 51 (2003), hep-ph/0306106
154. F. D. Steffen (2007), arXiv:0708.3600 [hep-ph]